J. Fluid Mech. (1987), *vol.* 184, *pp.* 245–266
Printed in Great Britain

Laminar-film condensation/evaporation on a vertically fluted surface

By R. E. JOHNSON

Department of Theoretical and Applied Mechanics, University of Illinois at Urbana-Champaign, Urbana, IL 61801, USA

AND A. T. CONLISK

Department of Mechanical Engineering, The Ohio State University, Columbus OH 43210, USA

(Received 4 November 1986 and in revised form 13 March 1987)

Laminar-film flow with condensation or evaporation on a vertical fluted cylinder is examined. A kinematic wave equation describing the evolution of the film profile is obtained and solutions presented. The film profile evolves owing to axial, gravity-driven flow and transverse, surface-tension-driven flow from the crests to the valleys of the fluted cylinder. In the case of condensation the majority of the film reaches a uniform thickness and consequently there is a significant improvement in heat transfer compared with the classical unfluted result where the film thickens in an unbounded fashion. For evaporation a critical value of a parameter which involves the ratio of the Weber number and the gradient of the surface curvature is found below which the film totally drys out and above which the fluid funnels into tapering rivulets and only partially drys out. Typical dry-out lines are presented. For short cylinders the evaporative mass transfer for a fluted cylinder is slightly greater than that predicted for an unfluted case. However, when the cylinder is long the mass transfer is far less for a fluted cylinder owing to the reduction in film area associated with partial film dry out.

1. Introduction

Since the pioneering work of Nusselt (1916) for smooth cylindrical surfaces and Gregorig (1954) for axially fluted surfaces, there has been a great deal of work done on laminar-flow condensation and evaporation on vertical surfaces. The results of Gregorig (1954) are especially significant since condensation rates were shown to be significantly enhanced compared with the results for a vertical cylindrical surface.

Despite the large amount of experimental and analytical work on the fluted surface problem, the reason for the large increase in condensation rate (and by analogy, the evaporation rate as well) is at present unknown (see, for example, Rothfus & Lavi (1978) for an excellent literature review on the subject; also several other articles in that volume are relevant). It is believed, however, that surface tension is crucial to the enhancement process although the evidence to support this view is still rather sketchy. The reason for this is that in the analytical work on this problem, simplifying assumptions have often been made regarding the shape of the film surface which renders precise interpretation of the results somewhat difficult (see Honda & Fujii 1984; Mori *et al.* 1979; Panchal & Bell 1979; Webb 1979; Sideman, Levin & Moalem-Maron 1982; Sideman & Levin 1979; and Joos 1984 for example). As a first step towards a detailed understanding of the flow and heat transfer as a function of

tube geometry (and hence prediction of condensation/evaporation rates), this paper is concerned with the calculation of the flow field on an axially fluted surface and the effect of surface tension on the fluid motion. The geometry of the problem is depicted in figure 1. Fluid enters at the top through a thin slot and passes vertically down the tube under the action of gravity; it emerges that at the crests the film surface thins in the axial direction because of drainage into the valleys of the flutes as is shown in the side view of figure 1. In the present paper, it will be assumed that the film thickness remains thin compared with the smallest lengthscale of the problem (i.e. flute spacing, for example). Bounding the liquid film is a gas, for example air, or the vapour associated with the liquid, for which the viscosity ratio $\mu_g/\mu_L \ll 1$, where μ_L and μ_g are the viscosities of the liquid and gas phase respectively; because $\mu_g/\mu_L \ll 1$, motion in the gas may be neglected to leading order. The Reynolds number based on characteristic film thickness h_0^*, $Re = \rho_L U h_0^*/\mu_L$ is assumed to be small enough that inertial effects may be neglected; the characteristic velocity in the film is defined as $U = \rho_L g h_0^{*2}/\mu_L$, where ρ_L is the density of the liquid and h_0^* is the dimensional inlet gap width at the top of the tube (i.e. a nominal film thickness).

The bulk of the previous work on the fluted-surface problem has been in the condensation area; it should be noted that the precise details of the three-dimensional, three-component fluid flow field which the fluted surface generates have largely been ignored. Honda & Fujii (1984) consider condensation on a fluted surface assuming a thin film on the crest and a thick film in the valley; the point of cross-over is determined by the condition that the interfacial curvature in the thick film is almost constant; the velocity field is not calculated. Mori *et al.* (1979) consider a similar problem, however there is an inconsistency in the film equation if the surface tension coefficient $\sigma \to 0$. The film is divided somewhat arbitrarily into three regions roughly corresponding to thick film, thin film and transition regions; moreover, the film surface in the thick film region is assumed to be a circular arc. The three-dimensional velocity field is also not calculated; similar comments apply to the work of Panchal & Bell (1979) and Sideman & Levin (1979), while Webb (1979) was concerned with an overall design process and so he did not consider the velocity and temperature fields at all. Sideman *et al.* (1982) assumes the vertical flow rate to be constant for low surface-tension values; the velocity in the axial direction is calculated numerically by a finite-difference scheme; however, the other two velocity components are not considered.

It should be pointed out that Joos (1984) has obtained solutions to the problem of film condensation on fluted surfaces for thin films using boundary-layer techniques and he obtains a thermal enhancement which increases in the axial direction and is dependent on the amplitude of the flutes; however, his notation obscures the results and the film profiles apparently have a discontinuity in slope which (the authors believe) is a result of a mistake in his calculations (see figures 2 and 8 of Joos 1984). Consequently, the enhancement factors that he quotes are not likely to be correct and it is the purpose of the present paper to clarify the condensation problem as well as to present results for the evaporation problem and the purely incompressible film problem. In §2 the governing equations for the present problem are given in a coordinate system with surface-fitted coordinates. In §3 solutions for the velocity field are given and in §4 the film profiles are obtained analytically for each of the three cases of condensation, evaporation and the purely incompressible liquid film without heat transfer. The behaviour of the solutions as a function of curvature is detailed and a suitable enhancement factor is defined for the two problems with heat transfer; for the case of evaporation, a dry-out length is calculated and it emerges

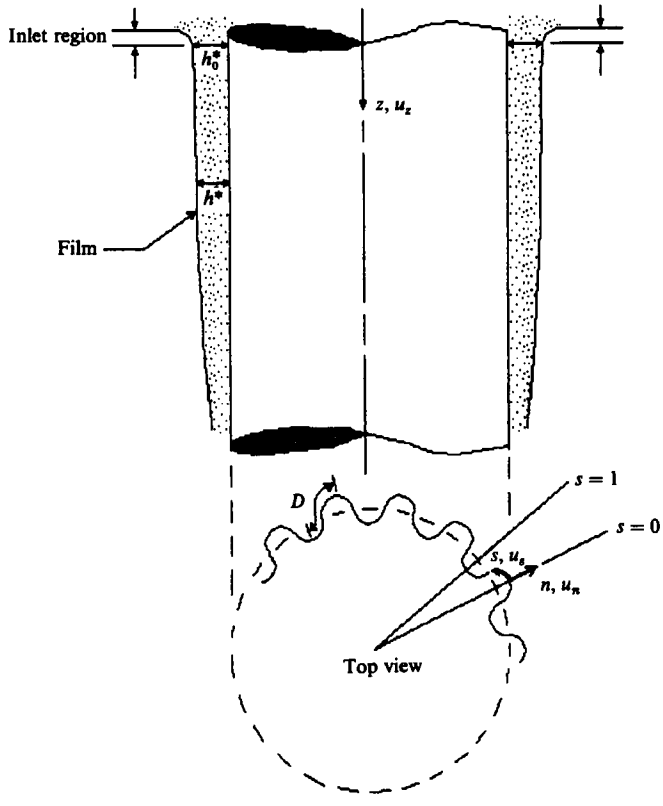

FIGURE 1. Schematic of the fluted tube geometry operating in the evaporation mode; both side and top views are shown. The condensation problem is similar except that the film thickness is zero at the inlet region. Dimensionless coordinates and velocities are shown.

that the film thickness vanishes first near the crest in a distance that depends crucially on the value of the surface-tension coefficient, the evaporation rate, the flute spacing, and the surface curvature gradient. Finally, in §5, the conclusions of the present study are given.

In what follows we shall see that the fluid is driven in the axial direction by gravity and that the relatively large interfacial curvature at the crests relative to the troughs will produce a pressure field driving a transverse flow of fluid from the crests to the troughs. For condensation we find that the film reaches a uniform thickness over the majority of the film surface except for a small region near the troughs which will steadily thicken owing to the inflow from the crests. This limiting film thickness over the majority of the film results in enhanced heat transfer compared with that for an unfluted cylinder. For evaporation we find that the thinning of the film at the crest is enhanced by a corresponding increased evaporation rate there, and the film ultimately drys out at the crests first. However, as we shall see, the trough region may or may not dry out depending on the parameters in a given problem. When the film does not dry out in the troughs, the fluid is found to funnel from the crests into tapering rivulets in the troughs which persist indefinitely in the axial direction.

2. Governing equations and boundary conditions

2.1. *Governing equations*

In this paper we consider the gravity-driven film flow down a fluted cylindrical surface in the geometry of figure 1. In order to simplify the analysis and deduce the basic structure of the flow with (and without) phase change, the Nusselt-type limit is considered whereby the convective terms in the Navier–Stokes equations are neglected. The liquid density is ρ_{L}, and g is the acceleration due to gravity. For convenience we use a surface-fitted orthogonal curvilinear coordinate system (n, s, z) where n is perpendicular to the cylinder surface, and s is arc length along the cylinder's perimeter. The curvature of the cylinder surface is $\kappa_b(s)$. The non-dimensional governing equations in the orthogonal (n, s, z) coordinate system (figure 1) are given by

$$\nabla^2 u_n + \frac{\delta}{f^3}\kappa_b' u_s + \frac{2\delta}{f^2}\kappa_b \frac{\partial u_s}{\partial s} - \frac{\delta^2\kappa_b^2}{f^2} u_n = \frac{We^{-1}}{\delta^2}\frac{\partial p}{\partial n}, \tag{1}$$

$$\nabla^2 u_s - \frac{\delta^3\kappa_b'}{f^3} u_n - \frac{2\delta^3\kappa_b}{f^2}\frac{\partial u_n}{\partial s} - \frac{\delta^2\kappa_b^2 u_s}{f^2} = We^{-1}\frac{\partial p}{\partial s}, \tag{2}$$

$$\nabla^2 u_z = -1 + We^{-1}\frac{\epsilon}{\delta}\frac{\partial p}{\partial z}, \tag{3}$$

where $\kappa_b' = \mathrm{d}\kappa_b/\mathrm{d}s$ and

$$\nabla^2 = \frac{\partial^2}{\partial n^2} - \frac{\delta\kappa_b}{f}\frac{\partial}{\partial n} + \frac{\delta^2}{f}\frac{\partial}{\partial s}\left(\frac{1}{f}\frac{\partial}{\partial s}\right) + \epsilon^2\frac{\partial^2}{\partial z^2},$$

$$f(s, n) = 1 - \delta n\kappa_b(s).$$

In (1)–(3) the velocity field $\boldsymbol{u}^* = (u_s^*, u_n^*, u_z^*)$ and pressure p^* are made dimensionless by

$$u_n = \frac{u_n^*}{\delta U}, \quad u_s = \frac{u_s^*}{U}, \quad u_z = \frac{u_z^*}{U}, \quad p = \frac{p^*}{\sigma/D}, \tag{4}$$

where the characteristic velocity $U = \rho_{\mathrm{L}} g h_0^{*2}/\mu_{\mathrm{L}}$, σ is the surface tension and

$$n = \frac{n^*}{h_0^*}, \quad s = \frac{s^*}{D}, \quad z = \frac{z^*}{L}, \quad \kappa_b = D\kappa_b^*, \tag{5}$$

where the asterisk denotes dimensional quantities. Here h_0^* is the nominal liquid film thickness, D the crest-to-trough distance on the fluted surface of the cylinder and L is a typical lengthscale in the z-direction which will emerge from the analysis shortly. Also,

$$We = \frac{\rho_{\mathrm{L}} g D^2}{\sigma}, \quad \delta = \frac{h_0^*}{D}, \quad \epsilon = \frac{h_0^*}{L} \tag{6}$$

are the three governing dimensionless parameters with We being the Weber number. In the subsequent analysis, δ and ϵ will be assumed small, i.e. the fluid layer is thin.

Equations (1)–(3) are supplemented by the continuity equation

$$\frac{\partial u_n}{\partial n} + \frac{1}{f}\frac{\partial u_s}{\partial s} - \frac{\delta\kappa_b}{f}u_n + \frac{\epsilon}{\delta}\frac{\partial u_z}{\partial z} = 0, \tag{7}$$

and the energy equation which is given by

$$\frac{\rho_{\mathrm{L}} C_{p\mathrm{L}} UD}{k_{\mathrm{L}}}\delta^2\left\{u_n\frac{\partial T}{\partial n} + \frac{u_s}{f}\frac{\partial T}{\partial s} + \frac{\epsilon}{\delta}u_z\frac{\partial T}{\partial z}\right\} = \frac{1}{f}\frac{\partial}{\partial n}\left(f\frac{\partial T}{\partial n}\right) + \frac{\delta^2}{f}\frac{\partial}{\partial s}\left(\frac{1}{f}\frac{\partial T}{\partial s}\right) + \epsilon^2\frac{\partial^2 T}{\partial z^2} = \nabla^2 T.$$

Here the temperature has been purposely left dimensional for reasons that will become clear subsequently. In what follows we shall neglect convective terms in the energy equation and restrict attention to

$$\nabla^2 T = 0. \tag{8}$$

This restriction is consistent with the Nusselt-type flow in a thin film if the Prandtl number $Pr = \mu_L C_{pL}/k_L$ is $O(1)$. Here C_{pL}, and k_L are the specific heat, and thermal conductivity of the liquid respectively. In addition, from the boundary condition at the free surface we shall see below that owing to the condensation/evaporation process $u_n = O(k_L \Delta T/\rho_L h_0^* \delta U h_{fg})$, where ΔT is the temperature difference across the film and h_{fg} is the latent heat. Consequently, a further restriction is implied by neglecting the convective term which involves the normal velocity component u_n. Namely, using the magnitude of u_n given above the convective term

$$\frac{\rho_L C_{pL} UD}{k_L} \delta^2 u_n \frac{\partial T}{\partial n}$$

in the energy equation will be small provided that $C_{pL} \Delta T/h_{fg}$ is small compared with unity. Generally, for thin films $C_{pL} \Delta T/h_{fg}$ is much less than 0.2 and so it is reasonable to restrict attention to conductive heat transfer.

2.2. *Boundary conditions*

The velocity boundary conditions at the surface of the fluted cylinder $n = 0$ (see figure 1) are

$$u_n = u_s = u_z = 0 \quad \text{at } n = 0. \tag{9}$$

Boundary conditions on the temperature will be assumed to be of the form

$$T = T_w, \quad \text{at } n = 0, \text{ for condensation/evaporation,} \tag{10}$$

where T_w is the (dimensional) temperature of the wall.

The conditions at the free surface $n = h(s, z) = h^*(s, z)/h_0^*$ involve balancing shearing and normal stresses there. Because the vapour stress is neglected, the film surface is a no-shear-stress boundary which requires

$$\tau_{sn} = \frac{\partial u_s}{\partial n} + \frac{\delta}{f}\left\{\delta \frac{\partial u_n}{\partial s} + \kappa_b u_s\right\} = 0, \tag{11a}$$

$$\tau_{nz} = \frac{\partial u_z}{\partial n} + \delta\epsilon \frac{\partial u_n}{\partial z} = 0, \tag{11b}$$

and the jump in the normal stress is proportional to the film surface curvature,

$$-p + 2\delta We\left\{\delta \frac{\partial u_n}{\partial n} - \delta \frac{\partial h}{\partial s}\frac{\partial u_s}{\partial n} - \epsilon \frac{\partial h}{\partial z}\frac{\partial u_z}{\partial n}\right\}$$

$$= -\frac{1}{|\nabla F|}\left\{\frac{\kappa_b}{f} - \frac{\delta}{f}\frac{\partial}{\partial s}\left(\frac{1}{f}\frac{\partial h}{\partial s}\right) - \frac{\epsilon^2}{\delta}\frac{\partial^2 h}{\partial z^2}\right\} + O\left(\delta^3, \epsilon^2\delta, \frac{\epsilon^4}{\delta}\right), \tag{12}$$

where $$|\nabla F| = \left\{1 + \left(\frac{\delta}{f}\frac{\partial h}{\partial s}\right)^2 + \left(\epsilon \frac{\partial h}{\partial z}\right)^2\right\}^{\frac{1}{2}}, \quad f = 1 - \delta n \kappa_b.$$

In (12) we have neglected the effect of vapour recoil, i.e. the contribution to the normal stress jump due to the jump in the momentum flux across the interface. This effect is generally believed to be of secondary importance in practical applications

of laminar-film condensation/evaporation owing to the relatively low condensation/evaporation rates involved.

At the interface, the boundary condition on the temperature is given by

$$T = T_{\text{sat}}, \quad n = h(s, z); \tag{13}$$

the cases of condensation/evaporation will be obtained according to whether $T_w < T_{\text{sat}}$ or $T_w > T_{\text{sat}}$. Finally, we shall have a kinematic boundary condition relating the normal component of velocity at the film surface to the condensation/evaporation rate. This will be discussed fully in §3.2.

It should be noted here that in the physical case of interest, fluid enters via a small slot at the top of the tube; there is an entrance length depending on the given inlet velocity distribution, in which the velocity distribution changes from its inlet profile to the Nusselt-type profile downstream. At the low flow rates considered here the entrance region will be relatively short; consequently, it will have little effect on the solution and will not be discussed further. In what follows, where required, we specify a film thickness at $z = 0$ which will correspond to the inlet to the Nusselt regime.

2.3. *Fluted surfaces*

The types of surfaces considered here are called fluted surfaces and the form of these surfaces will now be discussed. We basically wish to address the question: given a curvature $\kappa_b(s)$ what is the cross-sectional shape of the cylinder? Consider a curve describing the cross-sectional shape of the cylinder with parametric equations $x = x_0(s)$ and $y = y_0(s)$, then the curvature of the surface is given by

$$\left(\frac{\partial^2 x_0}{\partial s^2}\right)^2 + \left(\frac{\partial^2 y_0}{\partial s^2}\right)^2 = \kappa_b^2, \tag{14}$$

and from the definition of a unit tangent vector to the curve we have

$$\left(\frac{\partial x_0}{\partial s}\right)^2 + \left(\frac{\partial y_0}{\partial s}\right)^2 = 1. \tag{15}$$

Combining (14) and (15), ordinary differential equations may be obtained for x_0 and y_0 according to

$$\left.\begin{aligned} \left(\frac{\partial^2 x_0}{\partial s^2}\right)^2 - \kappa_b^2 \left\{1 - \left(\frac{\partial x_0}{\partial s}\right)^2\right\} = 0; \\ \left(\frac{\partial^2 y_0}{\partial s^2}\right)^2 - \kappa_b^2 \left\{1 - \left(\frac{\partial y_0}{\partial s}\right)^2\right\} = 0. \end{aligned}\right\} \tag{16}$$

Equations (16) may easily be integrated and the results are

$$\left.\begin{aligned} x_0 = \int_0^s \sin K(s)\, \mathrm{d}s + X_0, \\ y_0 = \int_0^s \cos K(s)\, \mathrm{d}s + Y_0, \end{aligned}\right\} \tag{17}$$

where

$$K(s) = \int_0^s |\kappa_b|\, \mathrm{d}s,$$

X_0 and Y_0 are the initial points of the curve at $s = 0$ and we have taken $\partial x_0/\partial s = 0$ and $\partial y_0/\partial s = 1$ at $s = 0$ for convenience.

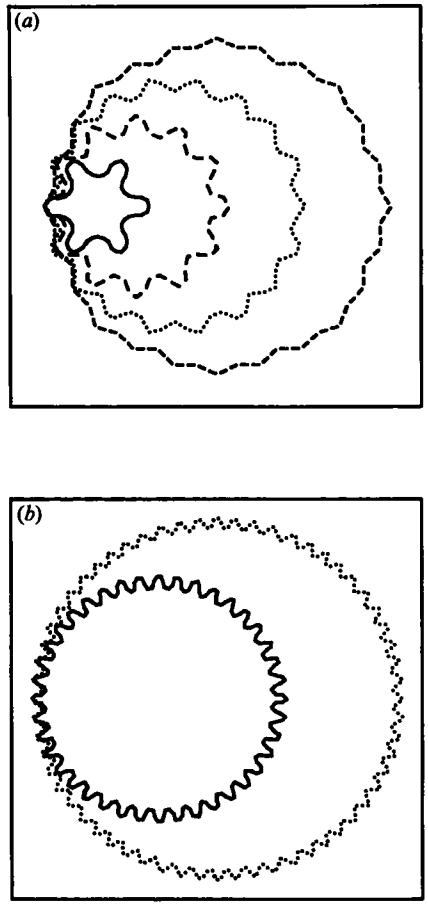

FIGURE 2. Fluted cylinder cross-sections: (*a*) $\kappa_0 = 4$ and $N = 6, 12, 18, 24$; (*b*) $\kappa_0 = 5$ and $N = 40, 60$.

The types of surfaces for which we shall present results later are those of the form

$$\kappa_b = \kappa_1 + \kappa_0 \cos \pi s, \tag{18}$$

where for a closed curve periodicity requires

$$\kappa_1 \frac{P_0^*}{D} = 2\pi,$$

where P_0^* is the dimensional perimeter and P_0^*/D must be an integer equal to twice the number of flutes, say $2N$ (recall that D is the crest-to-trough distance). Note that we have chosen the sign convention for the curvature such that κ_b is positive and clearly it is largest at the crests and smallest in the troughs. To illustrate the types of surfaces that are generated by (17) and (18), on figure 2 are plots of several surfaces for $\kappa_0 = 4$ and $N = 6, 12, 18, 24$ and for $\kappa_0 = 5$ and $N = 40, 60$. The amplitude of the flutes is governed, in part, by the parameter κ_0. As N increases, of course, D decreases for fixed mean radius and flute amplitude and for what follows, the number of flutes is limited by the requirement of a thin film (i.e. $\delta = h_0^*/D \ll 1$); typically we will find that $D < L$ and in applications N is usually less than 60.

3. Solutions for a thin film

3.1. *The velocity and temperature fields*

For a thin film $\delta, \epsilon \ll 1$ and (1) gives the usual leading-order result

$$\frac{\partial p}{\partial n} \approx 0, \quad p = p(s, z).$$

For the momentum equation in the axial direction, (3), we have, to leading order,

$$\frac{\partial^2 u_z}{\partial n^2} = -1 + \frac{\epsilon}{\delta} We^{-1} \frac{\partial p}{\partial z}, \tag{19}$$

and the solution, subject to $u_z = 0$, $n = 0$ and $\partial u_z/\partial n = 0$ at $n = h(s, z)$ (see (11*b*)) is given by

$$u_z = \left(-1 + \frac{\epsilon}{\delta} We^{-1} \frac{\partial p}{\partial z}\right)(\tfrac{1}{2}n^2 - nh). \tag{20}$$

Similarly from (2),

$$u_s = We^{-1} \frac{\partial p}{\partial s}(\tfrac{1}{2}n^2 - nh), \tag{21}$$

and the continuity equation determines u_n according to

$$u_n = -\int_0^n \left(\frac{\partial u_s}{\partial s} + \frac{\epsilon}{\delta} \frac{\partial u_z}{\partial z}\right) \mathrm{d}n, \tag{22}$$

where we have nominally assumed at this stage that $\epsilon/\delta \leqslant O(1)$.

The conduction-dominated temperature profile is easily obtained from (8) subject to boundary conditions (10) and (13) and the result is

$$T = (T_{\mathrm{sat}} - T_{\mathrm{w}}) \frac{n}{h} + T_{\mathrm{w}} \text{ for condensation/evaporation.} \tag{23}$$

At this point calculation of the film surface profile is considered.

3.2. *The film surface profile*

The solutions for the velocity and temperature fields are standard Nusselt-type solutions except that the film surface $h(s, z)$ is unknown. To find this, consider the vector normal to the fluid film surface which is given by

$$\boldsymbol{i}_n = \left(1, \; -\delta \frac{\partial h}{\partial s}, \; -\epsilon \frac{\partial h}{\partial z}\right)$$

at leading order. Using the kinematic condition that the component of velocity perpendicular to the film surface should equal the mass flux due to evaporation/condensation, we have

$$\frac{\boldsymbol{u}^*}{\delta U} \cdot \boldsymbol{i}_n = -\int_0^h \left(\frac{\partial u_s}{\partial s} + \frac{\epsilon}{\delta} \frac{\partial u_z}{\partial z}\right) \mathrm{d}n - \frac{\partial h}{\partial s} u_s - \frac{\epsilon}{\delta} u_z \frac{\partial h}{\partial z} = \frac{q}{\rho_{\mathrm{L}} h_{\mathrm{fg}} \delta U} \tag{24}$$

to leading order in δ, where h_{fg} is the heat of vaporization (condensation) and the dimensional heat flux at the surface is $q \approx -k_{\mathrm{L}} \partial T/\partial n^*$ at $n^* = h^*(s, z)$. From (23) for the temperature distribution

$$q = -k_{\mathrm{L}} \frac{\partial T}{\partial n^*}\bigg|_{n^* = h^*} = -\frac{k_{\mathrm{L}}}{h_0^*} \frac{\partial T}{\partial n} = -k_{\mathrm{L}} \frac{\Delta T}{h_0^* h}, \quad \Delta T = T_{\mathrm{sat}} - T_{\mathrm{w}}. \tag{25}$$

Note also that, in (24), convection of heat axially in the film has been neglected consistent with the thin-film assumption. The (dimensionless) liquid/vapour flux at the interface $\dot{m}$ is given by $q/\rho_L h_{fg}\delta U$ and in what follows $\dot{m}$ equals $-Q/h$, with $Q = k_L \Delta T/(\rho_L h_0^* \delta U h_{fg})$. In general, Q can be a function of s, z if, for example, the wall temperature in (25) $T_w = T_w(s, z)$.

Exchanging differentiation and integration using the Leibnitz rule, and performing the indicated integrations using (20) and (21) for u_z and u_s, the following partial differential equation for h^3 emerges from (24):

$$\frac{\epsilon}{\delta}\frac{\partial}{\partial z}\left[\left(1-\frac{\epsilon}{\delta}We^{-1}\frac{\partial p}{\partial z}\right)h^3\right]-We^{-1}\frac{\partial}{\partial s}\left(\frac{\partial p}{\partial s}h^3\right)=\frac{3Q}{h}. \tag{26}$$

We can now establish the previously unspecified characteristic lengthscale L in the axial direction. Since $\epsilon/\delta = D/L$, the lengthscale L over which h changes appreciably owing to transverse, surface-tension-driven flow is given by requiring a balance between the terms on the left-hand side of (26), i.e.

$$\frac{\epsilon}{\delta} = We^{-1} \quad \text{or } L = \frac{\rho g D^3}{\sigma} = WeD.$$

Moreover, since in practical application the surface-tension forces are weak compared with gravity forces, typically We^{-1} is small so that the axial pressure gradient in (26) may be neglected, and finally

$$\frac{\partial h^3}{\partial z}-\frac{\partial}{\partial s}\left(\frac{\partial p}{\partial s}h^3\right)=3We\frac{Q}{h}. \tag{27}$$

Equation (27) determines the film surface profile subject to an initial condition

$$h = h_1(s), \quad \text{at } z = 0. \tag{28}$$

The pressure $p(s, z)$ in (27) is determined by the normal stress boundary condition at the free surface, i.e. (12),

$$p \approx \frac{\kappa_b}{f}-\delta\frac{\partial^2 h}{\partial s^2}, \tag{29}$$

and consequently (27) becomes

$$\frac{\partial h^3}{\partial z}-\frac{\partial}{\partial s}\left[h^3\frac{\partial}{\partial s}\left(\frac{\kappa_b}{f}-\delta\frac{\partial^2 h}{\partial s^2}\right)\right]=3We\frac{Q}{h}. \tag{30}$$

For δ small, $f \sim 1 + O(\delta)$, and to leading order (30) becomes

$$\frac{\partial h^3}{\partial z}-\frac{\partial}{\partial s}\left[h^3\frac{\mathrm{d}\kappa_b}{\mathrm{d}s}\right]=3We\frac{Q}{h}. \tag{31}$$

Finally, writing $Q = Q_0\hat{Q}(s, z)$, where Q_0 is a constant equal to the nominal value of Q, and defining $h = (3Q_0 We)^{\frac{1}{3}}\hat{h}$ we write (31) as

$$\frac{\partial \hat{h}^3}{\partial z}-\frac{\partial}{\partial s}\left[\hat{h}^3\frac{\mathrm{d}\kappa_b}{\mathrm{d}s}\right]=\frac{\hat{Q}}{\hat{h}}. \tag{32}$$

Note that when $Q = \text{const}$ we shall have $\hat{Q} \equiv 1$. In the next section we discuss the solution for the cases of condensation, evaporation, and for no heat transfer.

4. Film profile solutions

4.1. *Condensation*

The solution to (32) for the film profile $h = (3Q_0\,We)^{\frac{1}{3}}\hat{h}(s,z)$ is conveniently obtained by rewriting (32) for $\hat{h}$ as

$$\frac{\partial \hat{h}^4}{\partial s} - \frac{1}{\kappa_b'}\frac{\partial \hat{h}^4}{\partial z} = -\frac{4}{3}\left(\frac{\hat{Q} + \hat{h}^4\kappa_b''}{\kappa_b'}\right), \tag{33}$$

which is easily identified as a kinematic wave equation (Whitham 1974). Consequently, using the notion of a total derivative, we rewrite this as an evolution equation for h along characteristic curves $z = z(s)$, i.e.

$$\frac{\mathrm{d}\hat{h}^4}{\mathrm{d}s} = -\frac{4}{3}\left(\frac{\hat{Q} + \hat{h}^4\kappa_b''}{\kappa_b'}\right) \tag{34a}$$

on curves prescribed by

$$\frac{\mathrm{d}z}{\mathrm{d}s} = -\frac{1}{\kappa_b'}. \tag{34b}$$

Furthermore, (34a) can be rewritten as

$$\frac{\mathrm{d}}{\mathrm{d}s}[(\kappa_b')^{\frac{4}{3}}\hat{h}^4] = -\tfrac{4}{3}\hat{Q}(\kappa_b')^{\frac{1}{3}} \tag{35}$$

and therefore, provided that $\kappa_b' \neq 0$, the film profile h is given along characteristic curves by

$$[(\kappa_b'(s))^{\frac{1}{3}}\hat{h}(s)]^4 - [(\kappa_b'(s_0))^{\frac{1}{3}}\hat{h}_1(s_0)]^4 = -\frac{4}{3}\int_{s_0}^{s} \hat{Q}(\bar{s}, z(\bar{s}))\,(\kappa_b'(\bar{s}))^{\frac{1}{3}}\,\mathrm{d}\bar{s}$$

or

$$\hat{h}^4(s) = \left(\frac{\kappa_b'(s_0)}{\kappa_b'(s)}\right)^{\frac{4}{3}}\hat{h}_1^4(s_0) - \frac{4}{3(\kappa_b'(s))^{\frac{4}{3}}}\int_{s_0}^{s} \hat{Q}(\bar{s}, z(\bar{s}))\,(\kappa_b'(\bar{s}))^{\frac{1}{3}}\,\mathrm{d}\bar{s} \tag{36a}$$

on curves

$$z = -\int_{s_0}^{s} \frac{\mathrm{d}\bar{s}}{\kappa_b'(\bar{s})}, \tag{36b}$$

where $s_0 = s_0(s,z)$ is the starting location of a characteristic at $z = 0$ which passes through s at z and $\hat{h}_1(s_0)$ is the initial value of $\hat{h}_1$ at the entrance $z = 0$. Note, however, that on surfaces where $\kappa_b'(s) = 0$ at one or more points (such as the crest or trough of the fluted surfaces of particular interest here), we must return to (32) to obtain the solution. In the present geometry $\kappa_b' = 0$ at $s = 0, 1$ and therefore the axial evolution of h for $s = 0, 1$ is given by

$$\frac{\partial \hat{h}^4}{\partial z} = \tfrac{4}{3}[\hat{Q}(s,z) + \hat{h}^4\kappa_{b_0}''], \tag{37}$$

where $\kappa_{b_0}'' = \kappa_b''(s = 0 \text{ or } 1)$ and the solution for $s = 0$ or 1 is

$$\hat{h}^4 = \exp[\tfrac{4}{3}\kappa_{b_0}'' z]\left\{\hat{h}_1^4(s,0) + \frac{4}{3}\int_0^z \hat{Q}(s,\bar{z})\exp[-\tfrac{4}{3}\kappa_{b_0}''\bar{z}]\,\mathrm{d}\bar{z}\right\}. \tag{38}$$

The preceding results are for surfaces of rather general cross-sectional shape and general condensation/evaporation rates. However, if we take Q to be constant, i.e.

$\hat{Q} = 1$, the initial film thickness to be zero, and consider fluted surfaces of the type described in §2.3 (equation (18)), then (36*a*, *b*) reduce to

$$\hat{h}(s) = \left(\frac{4}{3\pi\kappa_0}\right)^{\frac{1}{4}} \frac{\left[\int_{s_0}^{s} \sin^{\frac{1}{3}} \pi\bar{s}\, \mathrm{d}\bar{s}\right]^{\frac{1}{4}}}{\sin^{\frac{1}{3}} \pi s}, \tag{39a}$$

on curves

$$\pi^2\kappa_0 z = \ln\left\{\frac{\tan(\frac{1}{2}\pi s)}{\tan(\frac{1}{2}\pi s_0)}\right\}. \tag{39b}$$

Similarly, for $s = 0$ or 1, (38) becomes

$$\hat{h}^4 = -\frac{1}{\kappa''_{b_0}}\{1 - \exp[\tfrac{4}{3}\kappa''_{b_0} z]\}, \tag{40}$$

where $\kappa''_{b_0} = -\pi^2\kappa_0$ at the crests $s = 0$ and $\kappa''_{b_0} = +\pi^2\kappa_0$ at the troughs $s = 1$. Since $\kappa''_{b_0} < 0$ at the crest, the film thickens to an asymptotic value of $\hat{h} \to (-1/\kappa''_{b_0})^{\frac{1}{4}}$ as $z \to \infty$. At the trough $s = 1$, $\kappa''_{b_0} > 0$ and the film thickens exponentially as $z \to \infty$. The evolution of a generic film profile valid for all κ_0, Q_0 and We for this case is shown in figure 3 where we plot $H = (\frac{3}{4}\pi\kappa_0)^{\frac{1}{4}}\hat{h} = (\pi\kappa_0/4Q_0\, We)^{\frac{1}{4}}h$ versus s for a few values of $Z = \pi^2\kappa_0 z$. Note that the film profile plotted is for one segment of fluted cylinder (crest to trough) and therefore the pattern is repeated going around the fluted cylinder. Clearly as $z \to \infty$, the majority of the film tends to an asymptote, while in the immediate vicinity of the trough the film is thickening exponentially. This is in marked contrast to the well-known result for an unfluted cylinder where the film thickens everywhere without bound at a rate proportional to $z^{\frac{1}{4}}$. This feature, as we shall see below, is directly responsible for a net heat transfer enhancement associated with fluted cylinders, and it has not been clearly identified before.

The solution in the neighbourhood of the trough where the film is growing exponentially is clearly a source of non-uniformity in the present solution for sufficiently large Z. From figure 3 we see that this non-uniformity begins to manifest itself when $Z = \pi^2\kappa_0 z$ has a value of about 4.0 since $\partial H/\partial s$ is becoming large in the troughs. This is due in part to the omission of the order-δ term in the pressure-field equation (29). If we reinstate the term $\delta\,\partial^2 h/\partial s^2$ into the pressure field we can smear out the profile in the neighbourhood of the trough and extend the validity of the present solution. In addition, it is appropriate to include higher-order surface-tension effects associated with the fact that film surface curvature is no longer approximated by the cylinder curvature $\kappa_b(s)$. This boundary-layer analysis in the neighbourhood of $s = 1$ will be discussed in a separate paper. We do not, however, believe that the net heat transfer rate will be significantly affected by the modifications made to the film profile in this boundary layer.

For the condensation case under consideration, where the initial film thickness is zero, it is instructive to recast the film thickness in dimensional form in order to identify the characteristic film thickness. From the original formulation we have the dimensional film thickness given by

$$h^* = h_0^*\, h(s, Z) = h_0^*(3Q_0\, We)^{\frac{1}{4}}\hat{h}(s, Z),$$

where $Q_0 = k_{\mathrm{L}}\Delta T/\rho_{\mathrm{L}}\, h_0^*\, \delta U h_{\mathrm{fg}}$ and $We = \rho_{\mathrm{L}} g D^2/\sigma$. Consequently, we see that

$$h^* = D[k_{\mathrm{L}}\Delta T\,\mu_{\mathrm{L}}/\rho_{\mathrm{L}}\, D h_{\mathrm{fg}}\,\sigma]^{\frac{1}{4}}\hat{h}(s, Z)$$

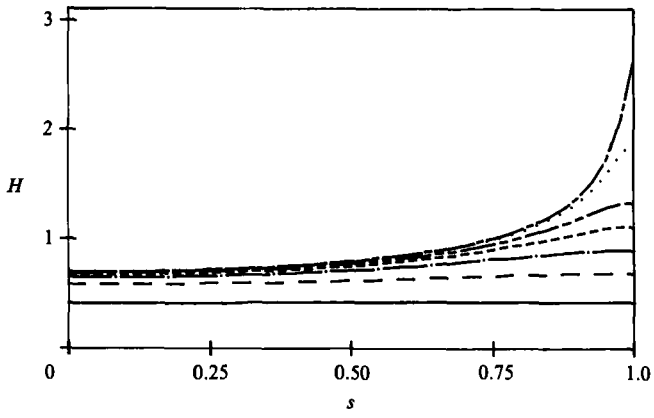

FIGURE 3. Condensation film profiles versus s for seven axial locations. Initial thickness $h_i = 0$ and constant wall temperature ($\gamma = 0$). ——, $Z = 0.1$; — — —, 0.5; —·—, 1.0; – – –, 1.5; — — —, 2.0; ·····, 3.0; ——, 4.0.

and therefore the characteristic film thickness can be written as

$$D\left[\frac{k_{\mathrm{L}}}{\rho_{\mathrm{L}} C_{p\mathrm{L}} D(\sigma/\mu_{\mathrm{L}})} \frac{C_{p\mathrm{L}} \Delta T}{h_{\mathrm{fg}}}\right]^{\frac{1}{4}},$$

where $\rho_{\mathrm{L}} C_{p\mathrm{L}} D(\sigma/\mu_{\mathrm{L}})/k_{\mathrm{L}}$ is a Péclet number based on the velocity scale σ/μ_{L} and $C_{p\mathrm{L}} \Delta T/h_{\mathrm{fg}}$ is a measure of the subcooling. From this we can also estimate the axial position along the cylinder where the growing film will violate the thin-film assumption $h^*/D \ll 1$. From the above we see that the present solution is valid provided that

$$[k_{\mathrm{L}} \Delta T \mu_{\mathrm{L}}/\rho_{\mathrm{L}} D h_{\mathrm{fg}} \sigma]^{\frac{1}{4}} \hat{h}(s, Z) \ll 1.$$

Examining this in the troughs where the film is growing exponentially, we have

$$\hat{h}^4 = -\frac{1}{\pi^2 \kappa_0}\{1 - \exp[\tfrac{4}{3}Z]\}$$

from (40) and we find that the thin-film assumption will be satisfied for axial positions that satisfy

$$Z = \pi^2 \kappa_0 z < O\left\{\tfrac{3}{4} \ln\left[1 + \frac{\rho_{\mathrm{L}} D h_{\mathrm{fg}} \sigma \kappa_0 \pi^2}{k_{\mathrm{L}} \Delta T \mu_{\mathrm{L}}}\right]\right\}.$$

As expected, if the temperature difference ΔT is large, the condensation rate is high and the solution is restricted to relatively small Z. In applications the working fluid is often ammonia (see Owens 1978 for a complete list of physical properties) and we have calculated for this case the limiting value of z^* for validity of the thin-film assumption based on a saturation temperature of 294.4 K, $\Delta T = 0.5$ K and $D = 14$ mm (0.55 in.). For ammonia, this choice for D corresponds to a length $L = WeD = 0.75$ m (2.46 ft). Therefore for $\kappa_0 = 1$ we find $z^* = zL \lesssim 1.42$ m (4.66 ft) and as κ_0 increases, the restriction becomes much more severe. For example, for $\kappa_0 = 5$ we find $z^* < 0.3$ m (1 ft). Note that these results are only weakly dependent on ΔT, but are strongly dependent on D.

Results for a second case corresponding to a variable wall temperature of the form $T_{\mathrm{w}} = T_{\mathrm{w}_0} + \Delta T_{\mathrm{w}} \cos \pi s$ are shown in figure 4. Here T_{w_0} is the mean wall temperature and we take $\Delta T_{\mathrm{w}} > 0$ so that the troughs are cooler than the crests. This particular

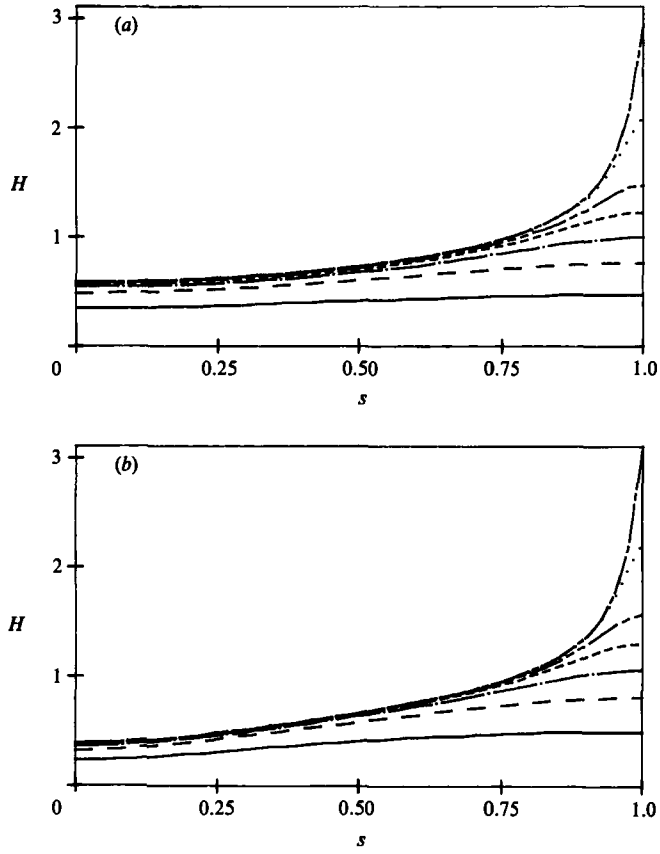

FIGURE 4. Condensation film profiles versus s for seven axial locations. Initial thickness $h_i = 0$ and variable wall temperature: (*a*) $\gamma = 0.5$, (*b*) $\gamma = 0.9$. ——, $Z = 0.1$; — — —, 0.5; —·—, 1.0; – – – –, 1.5; — — —, 2.0; · · · · ·, 3.0; — — —, 4.0.

choice for the temperature variation is motivated by the fact that the coolant flowing inside the fluted cylinder would more effectively cool the troughs, which appear as crests to the coolant inside the cylinder. Corresponding to this choice for wall temperature variation we have $Q = Q_0(1-\gamma\cos\pi s)$ where we define $Q_0 = k_L(T_{sat}-T_{w_0})/\rho_L h_0^* \delta U h_{fg} > 0$ and $\gamma = \Delta T_w(T_{sat}-T_{w_0}) > 0$. For condensation over the entire film surface we restrict attention to values of γ less than unity. In this case the film again starts with zero thickness at the entrance, but experiences (for $\gamma > 0$) decreased deposition of liquid into the film owing to condensation at the crests and an increase in the troughs. It should be pointed out that for this case Joos (1984) presented results from a similar solution obtained using a boundary-layer formulation, but his results show a spike in the film profile in the interior $0 < s < 1$ which travels from crest to trough as z increases (see Joos 1984, figure 2*b*); note that our results do not show this spike, and it is the present authors' conviction that there is an error in Joos' results. Comparing figures 3 and 4, it is clear that a substantial temperature variation is required in order to significantly modify the film profile.

The heat transfer from one segment of fluted surface between $s^* = 0$ and D, and $z^* = 0$ and z^* is given by

$$Q^* = k_L \int_0^D \int_0^{z^*} \frac{\partial T}{\partial n^*} \mathrm{d}z^* \, \mathrm{d}s^*, \tag{41}$$

where all quantities are dimensional at this stage. The total heat transfer from the cylinder between $z^* = 0$ and z^* equals $2NQ^*$, where N is the number of flutes. We now cast this result in terms of non-dimensional variables and since the z-dependence enters in the combination $\pi^2\kappa_0 z$ we introduce $Z = \pi^2\kappa_0 z = \pi^2\kappa_0 z^*/L$ (see, for example, (39b) or (40)). Consequently, for the case of uniform wall temperature we obtain

$$Q^* = \frac{k_L \Delta T D L}{h_0^* \pi^2 \kappa_0} \int_0^1 \int_0^Z \frac{\mathrm{d}Z\,\mathrm{d}s}{h(s,Z)}. \tag{42}$$

Furthermore, motivated by the solution for $h(s,Z)$, we write

$$h(s,Z) = \left(\frac{4Q_0 We}{\pi\kappa_0}\right)^{\frac{1}{4}} H(s,Z) \tag{43}$$

and using the relations $Q_0 = k_L \Delta T/\rho_L h_0^* \delta U h_{fg}$, $U = \rho_L g h_0^{*2}/\mu_L$ and $L = WeD$, we obtain

$$Q^* = \frac{k_L \Delta T D}{(4\pi)^{\frac{1}{4}}} \left(\frac{\rho_L^2 g h_{fg}}{\mu_L k_L \Delta T}\right)^{\frac{1}{4}} \left(\frac{L}{\pi^2\kappa_0}\right)^{\frac{3}{4}} \int_0^1 \int_0^Z \frac{\mathrm{d}Z\,\mathrm{d}s}{H(s,Z)}. \tag{44}$$

The corresponding well-known classical result due to Nusselt for an unfluted surface and uniform wall temperature ($\gamma = 0$) is given by

$$Q_{Nu}^* = \frac{4^{\frac{3}{4}}}{3} k_L \Delta T D \left(\frac{\rho_L^2 g h_{fg}}{\mu_L k_L \Delta T}\right)^{\frac{1}{4}} (z^*)^{\frac{3}{4}},$$

where $z^* = Lz = (L/\pi^2\kappa_0) Z$. Note that this classical result is readily obtained from (44) using $H(s,z)$, which follows from the solution of (32) taking $\kappa_b' \equiv 0$, i.e. assuming no flutes. Finally, an enhancement factor may be defined as

$$\alpha_c = \frac{Q^*}{Q_{Nu}^*} = \frac{3}{4\pi^{\frac{1}{4}}} \frac{1}{Z^{\frac{3}{4}}} \int_0^1 \int_0^Z \frac{\mathrm{d}Z\,\mathrm{d}s}{H(s,Z)}. \tag{45}$$

More generally, if we include variable wall temperature then taking account of this fact in (41), we now obtain

$$\begin{aligned} Q^* &= \frac{k_L (T_{sat} - T_{w_0}) D L}{h_0^* \pi^2 \kappa_0} \int_0^1 \int_0^Z \frac{(1 - \gamma \cos \pi s)}{h(s,Z)} \mathrm{d}Z\,\mathrm{d}s \\ &= \frac{k_L (T_{sat} - T_{w_0}) D}{(4\pi)^{\frac{1}{4}}} \left[\frac{\rho_L^2 g h_{fg}}{\mu_L k_L (T_{sat} - T_{w_0})}\right]^{\frac{1}{4}} \left[\frac{L}{\pi^2\kappa_0}\right]^{\frac{3}{4}} \int_0^1 \int_0^Z \frac{(1 - \gamma \cos \pi s)}{H(s,Z)} \mathrm{d}Z\,\mathrm{d}s. \end{aligned} \tag{46a}$$

In addition, if we include variable wall temperature in the classical unfluted result then the film thickness for an unfluted cylinder having zero initial film thickness may be written in the present notation as

$$H_{Nu} = \left[(1 - \gamma \cos \pi s) \frac{Z}{\pi}\right]^{\frac{1}{4}}.$$

Consequently, the rate of heat transfer for this slightly modified classical case is given by Q^* above, replacing $H(s,Z)$ with $H_{Nu}(s,Z)$, and we obtain an enhancement factor

$$\alpha_c = \frac{Q^*}{Q_{Nu}^*} = \frac{3}{4\pi^{\frac{1}{4}}} \frac{1}{Z^{\frac{3}{4}}} \frac{\displaystyle\int_0^1 \int_0^Z \frac{(1 - \gamma \cos \pi s)}{H(s,Z)} \mathrm{d}Z\,\mathrm{d}s}{\displaystyle\int_0^1 (1 - \gamma \cos \pi s)^{\frac{3}{4}} \mathrm{d}s}, \tag{46b}$$

where $H(s,Z)$ is the film thickness profile function for the fluted cylinder of interest.

Now for the fluted surfaces given by (18) and the special case when the film has zero initial thickness and $\hat{Q} = 1-\gamma\cos\pi s$ corresponding to the case of variable wall temperature discussed earlier, we have from (36*a*) and (43)

$$H(s,Z) = \frac{\left[\int_{s_0(s,Z)}^{s} (1-\gamma\cos\pi s')\sin^{\frac{1}{3}}\pi s'\,\mathrm{d}s'\right]^{\frac{1}{4}}}{\sin^{\frac{1}{3}}\pi s}, \tag{47}$$

where $s_0(s,Z)$ can be obtained from the equation for the characteristic curves (39*b*) and $\gamma = 0$ yields the constant-wall-temperature case.

The integral term appearing in (44) for constant wall temperature ($\gamma = 0$) and (46*a*) for variable wall temperature,

$$F(Z) = \int_0^1 \int_0^Z \frac{(1-\gamma\cos\pi s)}{H(s,Z)}\,\mathrm{d}Z\,\mathrm{d}s$$

is plotted in figure 5 versus $Z = \pi^2\kappa_0 z^*/L$ for the fluted surface given by (18) for constant wall temperature and for the two temperature variations considered previously (see figure 4), i.e. $\gamma = 0.5$ and 0.9. Since the film tends to one having a nearly uniform thickness over the majority of the film, we see that as Z gets large, $F(Z)$ and consequently, Q^* grow linearly. Therefore, since

$$Z = \pi^2\kappa_0 z^*/We\,D = (\pi^2\kappa_0\sigma/\rho_L g D^3)\,z^*,$$

if we consider a cylinder of fixed length z^*, then increasing κ_0, decreasing D, or increasing surface tension all increase the net heat transfer rate by increasing Z. The corresponding enhancement factors α_c for these cases are shown in figure 6. Note that α_c starts at unity at $Z = 0$ since the fluted film profile asymptotes to its unfluted counterpart for small Z, and that the enhancement increases most rapidly for moderate Z, but then increases more slowly. Consequently, increasing Z (by increasing κ_0, σ, or z^*, or by decreasing D) has its greatest payoff early and although increasing Z continues to improve the enhancement, the rate of improvement diminishes. For example, all other things being equal, increasing the cylinder length z^* is likely to have a practical limit with regard to improving the overall design. Note also that values of α_c as large as 5 can be found in the literature. From the present results it is quite apparent that α_c will attain a value of 5 at a very large value of Z and therefore it is somewhat impractical to numerically evaluate the value of Z where $\alpha_c = 5$ since this involves marching numerically forward in Z. However, since $F(Z)$ is very nearly linear for Z greater than about two we can easily extrapolate the values of $F(Z)$ for large Z using linear regression and thereby estimate α_c. From a linear regression using data for F between $Z = 10$ and 40, we find $F = 1.149\,Z + 0.873$ and consequently $\alpha_c = 2.06$ at $Z = 100$, $\alpha_c = 3.64$ at $Z = 1000$, and $\alpha_c = 5.15$ at $Z = 4000$ (note that the correlation coefficient for the fit was extremely close to unity, indicating a near perfect fit to a straight line).

4.2. *Evaporation*

The case of evaporation is similar except that $Q < 0$ and there will be a finite film thickness at the inlet to the tube. If we again consider variable wall temperature it is appropriate here to consider the troughs to be hotter than the crests and so we take $T_w = T_{w_0} - \Delta T_w\cos\pi s$ where ΔT_w is positive. The troughs are hotter than the crests in this case because we imagine that the hot working fluid inside the fluted

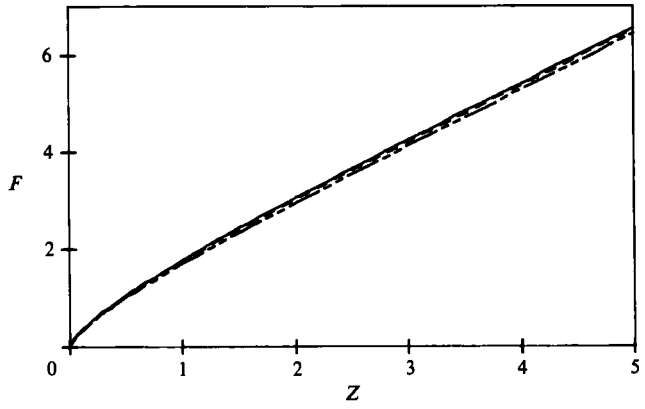

FIGURE 5. Heat transfer parameter $F(Z)$ for condensation on a fluted cylinder. Wall temperature variations: ——, $\gamma = 0$ (constant wall temperature); – – – –, 0.5; — — —, 0.9.

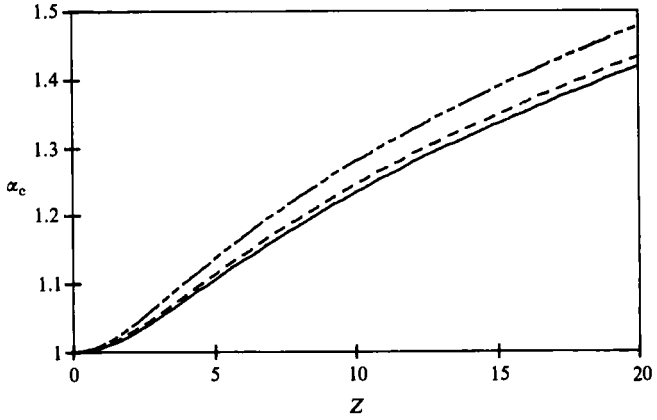

FIGURE 6. Heat transfer enhancement α_c versus Z for condensation. Wall temperature variations: ——, $\gamma = 0$ (constant wall temperature); – – – –, 0.5; — — —, 0.9.

cylinder heats the troughs more effectively since they appear as crests on the inside of the cylinder. With this choice we then have

$$Q = -Q_0(1-\gamma\cos\pi s),$$

where we now take

$$Q_0 = \frac{k_L(T_{w_0}-T_{sat})}{\rho_L h_0^* \delta U h_{fg}} > 0, \quad \gamma = \frac{\Delta T_w}{T_{w_0}-T_{sat}} > 0.$$

For the fluted surfaces given by (18), uniform initial film thickness and $Q = -Q_0(1-\gamma\cos\pi s)$ the film thickness is given by

$$h(s,Z) = \left(\frac{4Q_0\,We}{\pi\kappa_0}\right)^{\frac{1}{4}} H(s,Z)$$

with

$$H(s,Z) = \frac{\left[H_1^4 \sin^{\frac{4}{3}}\pi s_0 - \int_{s_0(s,Z)}^{s} (1-\gamma\cos\pi s')\sin^{\frac{1}{3}}\pi s'\,ds'\right]^{\frac{1}{4}}}{\sin^{\frac{1}{3}}\pi s}, \tag{48}$$

for $0 < s < 1$ where $s_0(s, Z)$ is again given by $Z = \ln\{\tan(\frac{1}{2}\pi s)/\tan(\frac{1}{2}\pi s_0)\}$, and at the crests $s = 0$, and troughs $s = 1$, we have respectively

$$H(0, Z) = \left(\frac{3}{4\pi}\right)^{\frac{1}{4}} [(1-\gamma+\tfrac{4}{3}\pi H_i^4)\exp(-\tfrac{4}{3}Z)-(1-\gamma)]^{\frac{1}{4}}, \tag{49a}$$

$$H(1, Z) = \left(\frac{3}{4\pi}\right)^{\frac{1}{4}} [1+\gamma-(1+\gamma-\tfrac{4}{3}\pi H_i^4)\exp(\tfrac{4}{3}Z)]^{\frac{1}{4}}. \tag{49b}$$

In the above expressions $H_i = (\pi\kappa_0/4Q_0\,We)^{\frac{1}{4}}h_i$ and it is appropriate to take the characteristic film thickness h_0^* equal to the initial thickness and hence $h_i = 1$.

From (49*a*) we see that dry out or vanishing of the film occurs at the crests at a distance

$$Z = \pi^2\kappa_0 z = \tfrac{3}{4}\ln\left[\frac{1-\gamma+\frac{4}{3}\pi H_i^4}{1-\gamma}\right]$$

(note that to have evaporation over the entire film $\gamma < 1$). On the other hand, dry out at the troughs will only occur for $H_i < [3(1+\gamma)/4\pi]^{\frac{1}{4}}$ in which case the film will vanish in the troughs at

$$Z = \tfrac{3}{4}\ln\left[\frac{1+\gamma}{1+\gamma-\frac{4}{3}\pi H_i^4}\right].$$

Consequently, the entire film vanishes only when

$$H_i < [3(1+\gamma)/4\pi]^{\frac{1}{4}} = 0.6990(1+\gamma)^{\frac{1}{4}}.$$

The dry out or contact lines $Z_d(s)$ computed by evaluating $H(s, Z_d) = 0$ from (48) for a few cases of H_i are shown for constant wall temperature ($\gamma = 0$) in figure 7. A rough sketch of how the film might appear on a fluted cylinder is shown in figure 8. Note that when total dry out does not occur the film drys out at the crests and the fluid funnels into tapering rivulets in the troughs. Corresponding film profiles $H(s, Z)$ are shown in figure 9 for two values of H_i one below the critical value resulting in total dry out ($H_i = 0.66$) and one above the critical value in which case total dry out does not occur ($H_i = 1.0$). In the case when total dry out occurs ($H_i = 0.66$, figure 9*a*) notice that the film steadily thins from its initial thickness uniformly over the film. In contrast, when the film only partially drys out ($H_i = 1.0$, figure 9*b*) we find the usual exponential thickening of the film in the troughs near $s = 1$ and thinning and dry out starting at the crests. Note also that this general dry-out behaviour is markedly different from the dry out of a film on an unfluted cylinder where for constant wall temperature $H_{Nu} = [H_i^4 - Z/\pi]^{\frac{1}{4}}$ and consequently total dry out always occurs at $Z = \pi H_i^4$. The film on a fluted cylinder drys out at the crest first and this point always occurs before the dry-out point on an unfluted cylinder owing to the exponential thinning of the film at the crest of a fluted cylinder. Furthermore, the film at the trough of a fluted cylinder will always extend beyond the dry-out point $Z = \pi H_i^4$ for an unfluted cylinder.

To cast the evaporation dry-out-line results in physical terms recall the definitions of H_i and Z,

$$H_i = \left(\frac{\pi\kappa_0}{4Q_0\,We}\right)^{\frac{1}{4}}, \quad Z = \frac{\pi^2\kappa_0}{We}\frac{z^*}{D}. \tag{50}$$

Therefore, the physical location of the dry-out or contact lines can be expressed as

$$\frac{z_d^*}{D} = \frac{We}{\pi^2\kappa_0} Z_d\left(\frac{s^*}{D}; H_i\right), \tag{51}$$

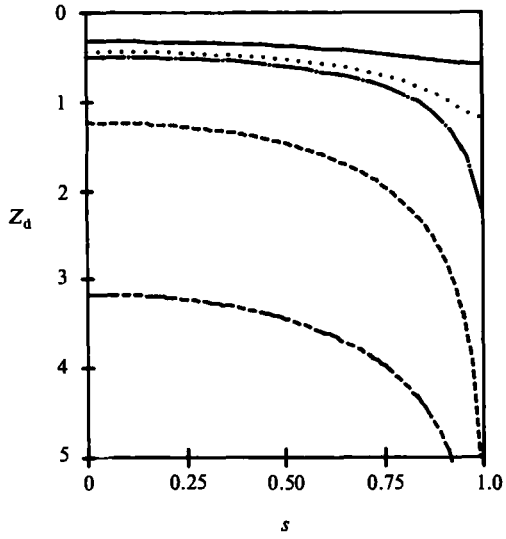

FIGURE 7. Dry-out lines for evaporation on a fluted cylinder ($\gamma = 0$), i.e. curves $Z_d(s)$ where the film thickness vanishes (note Z is plotted down in the direction of motion of the falling film). Evaporating film parameters $H_i = (\pi\kappa_0/4Q_0\,We)^{\frac{1}{4}}$: ——, $H_i = 0.6$; · · · · · · · · ,0.66; — · —,0.69; – – – –, 1.0; — — — —, 2.0.

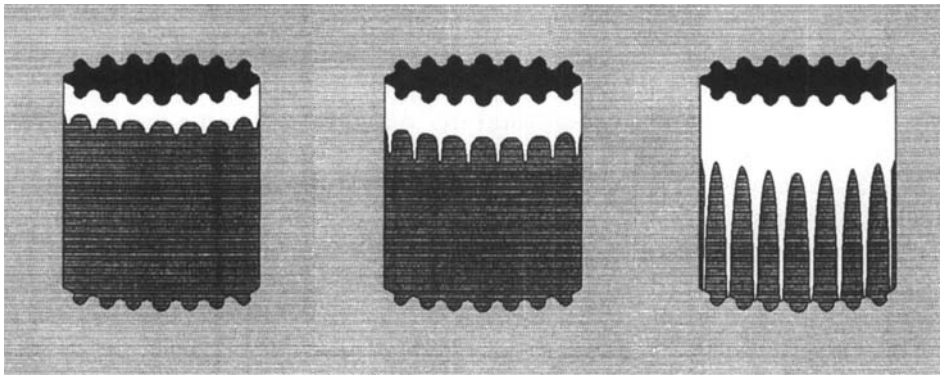

FIGURE 8. A sketch of the dry-out character of evaporating films (see also figure 7). The two figures on the left show films that totally dry out and the figure on the right shows the tapering rivulet formation.

where $H_i = (\pi\kappa_0/4Q_0\,We)^{\frac{1}{4}}$, $Q_0 = k_L\,\Delta T/\rho_L\,h_0^*\,\delta U h_{fg}$ and Z_d is a function of position s and the quantity H_i termed the evaporating film parameter (figure 7). Small H_i and consequently total dry out corresponds to small curvature gradient κ_0, large Weber number or small surface tension σ, and large mass transfer rate Q_0 or temperature difference ΔT. Partial dry out and rivulet formation results for values of H_i greater than 0.6990 (when $\gamma = 0$) and results from large κ_0 or σ and small mass transfer rate Q_0. Furthermore, from (51) we see that the absolute position of the dry-out line scales with We/κ_0.

For evaporation we can also identify an enhancement parameter α_e for one flute segment, namely, the ratio of the liquid masses evaporated up to a point z^* for a fluted and unfluted cylinder. Consequently, it is similar to the condensation case, (45, 46b)

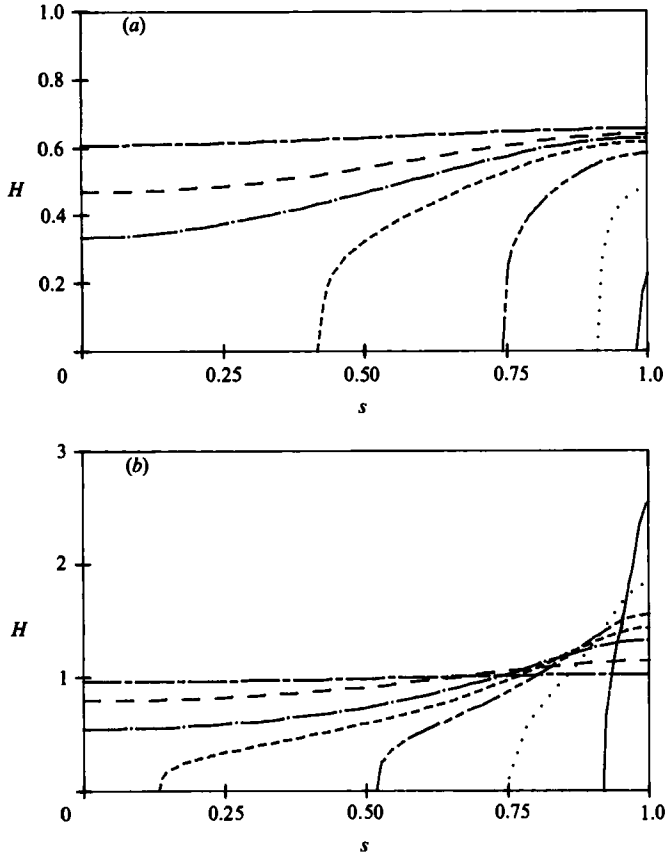

FIGURE 9. Evaporation film profiles versus s for seven axial locations and constant wall temperature ($\gamma = 0$). (*a*) $H_1 = 0.66$ and ——, $Z = 0.1$; — — —, 0.3; —·—, 0.4; – – –, 0.5; — — —, 0.7; · · · · · · ·, 1.0; ——, 1.18. (*b*) $H_1 = 1.0$ and ——, $Z = 0.1$; — — —, 0.5; —·—, 1.0; – – –, 1.25; — — —, 1.50; · · · · · · ·, 2.0; ——, 3.0.

except that the integration is only over the wetted portion of the cylinder surface. For constant wall temperature ($\gamma = 0$) we have,

$$\alpha_e = \frac{3}{4\pi^4}\frac{1}{Z^{\frac{3}{4}}}\int_0^Z \int_{s_d(Z)}^1 \frac{ds\,dZ}{H(s,Z)}, \tag{52}$$

where $s_d(Z)$ is the dry-out curve as a function of Z (the inverse of $Z_d(s)$ plotted in figure 7). Note that for points Z beyond where the film on an unfluted cylinder totally drys out, i.e. $Z = \pi H_1^4$, the quantity α_e is not defined. Also, in the case of evaporation, the significance of the enhancement parameter α_e becomes less clear than for condensation. For example, if the net heat transfer is the primary concern one should account for the heat transfer from the dry regions of a partially dried out film on a fluted cylinder. Nonetheless the behaviour of α_e is still worth exploring and it is plotted in figure 10 for one case which totally drys out ($H_1 = 0.66$) and for two other flute cases which do not totally dry out ($H_1 = 0.85$ and 1.0). In each case the enhancement parameter is greater than one up to the point where the fluted film partially drys out. After that point α_e drops below one and the mass transfer is less than that predicted by the classical unfluted theory. Initially α_e is greater than one

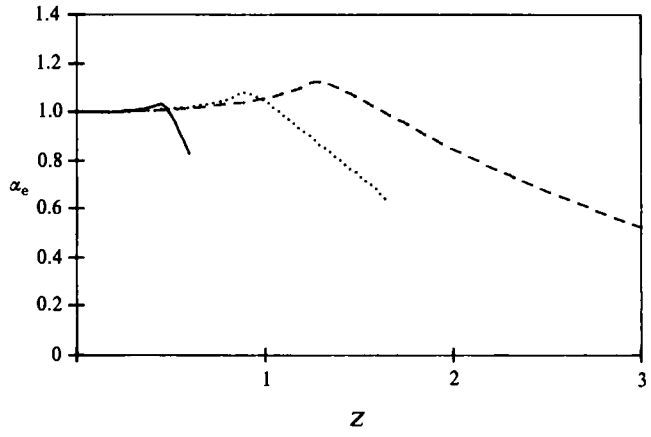

FIGURE 10. Mass transfer enhancement α_e versus Z for evaporation. Constant wall temperature and evaporating film parameters: ——, $H_i = 0.66$; ·····, 0.85; — — —, 1.0.

because over the majority of the fluted cylinder the film thins more rapidly than does a film on an unfluted surface. The only exception, of course, is close to the troughs where the film grows more rapidly. However, overall there is a net enhancement in mass transfer. Once the film on a fluted cylinder partially drys out then there is less surface area and a significant portion of the remaining film is thicker than the corresponding unfluted cylinder film. Consequently, α_e decreases fairly rapidly. Since the unfluted film drys out at $Z = \pi H_i^4$, α_e in figure 10 is not defined beyond $Z = 0.5961$ when $H_i = 0.66$, and $Z = 1.6399$ when $H_i = 0.85$, i.e. the last point plotted in each case, and $Z = \pi$ when $H_i = 1.0$. Note also that in the fluted case with $H_i = 0.66$ total dry out is completed in the troughs at $Z = 1.188$ (see figure 7), i.e. the troughs dry out well beyond where its unfluted counterpart totally drys out (the other two cases do not totally dry out).

4.3. *No heat transfer*

In this case $Q = 0$ and (36) gives

$$\hat{h} = \left(\frac{\kappa_b'(s_0)}{\kappa_b'(s)}\right)^{\frac{1}{3}} \hat{h}_i(s_0) \quad \text{on } z = -\int_{s_0}^{s} \frac{\mathrm{d}s}{\kappa_b'} \tag{53}$$

for $0 < s < 1$ and

$$\hat{h} = \hat{h}_1 \exp\left[\tfrac{1}{3}\kappa_{b_0}'' z\right] \tag{54}$$

for $s = 0, 1$. For the fluted cylinder we therefore have

$$\hat{h} = \left(\frac{\sin \pi s_0}{\sin \pi s}\right)^{\frac{1}{3}} \hat{h}_i(s_0) \quad \text{on } \pi^2 \kappa_0 z = \ln\left\{\frac{\tan\left(\frac{1}{2}\pi s\right)}{\tan\left(\frac{1}{2}\pi s_0\right)}\right\} \tag{55}$$

for $0 < s < 1$ and

$$\left.\begin{aligned} \hat{h}(0, z) &= \hat{h}_i(0, 0) \exp\left[-\tfrac{1}{3}\pi^2 \kappa_0 z\right], \\ \hat{h}(1, Z) &= \hat{h}_i(1, 0) \exp\left[\tfrac{1}{3}\pi^2 \kappa_0 z\right]. \end{aligned}\right\} \tag{56}$$

The film profile for $\hat{h}_i = 1$ is shown in figure 11 for a few values of $Z = \pi^2 \kappa_0 z$. The film becomes exponentially thin at the crest but never drys out. In practice one would expect short-range forces to play a role when the film gets sufficiently thin and dry out would probably occur.

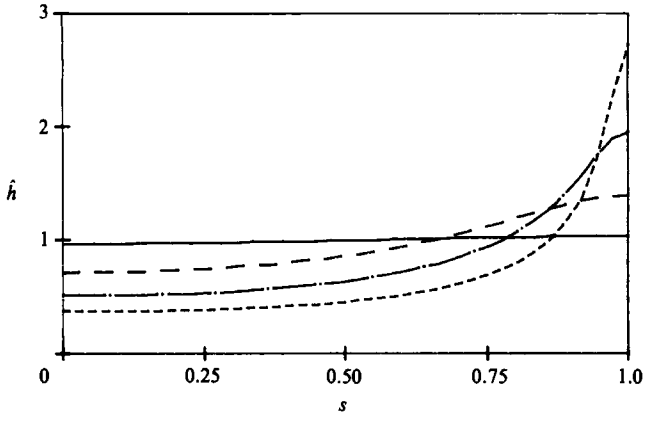

FIGURE 11. Film profiles without condensation/evaporation and initial thickness $h_1 = 1.0$. ——, $Z = 0.1$; ——, 1.0; —·—, 2.0; – – – –, 3.0.

5. Summary and conclusions

We have examined the flow and heat transfer in laminar-film condensation/evaporation on vertical surfaces with curvature-induced transverse surface tension flow. The relatively high curvature on the crests relative to the troughs produces a pressure field that drives fluid from the crests to the troughs. Consequently the film generally readjusts itself, becoming thicker in the troughs and thinner at the crests. For condensing films on fluted surfaces the film thickens and reaches an asymptotic thickness over the majority of the film surface. This limiting film thickness results in a significant heat transfer enhancement compared to Nusselt's classical result for unfluted surfaces. In the troughs the film generally thickens exponentially and provides an efficient flow path for the condensate. For an evaporating film, the transverse surface-tension flow, which is thinning the film at the crests, is reinforced by the increased evaporation rate at the crests due to the film thinning. This enhanced evaporation rate at the crests ultimately leads to dry out of the film at the crests. Furthermore, we find that during evaporation of a film for which $(\pi\kappa_0/4Q_0\,We)^{\frac{1}{4}} < 0.6990\,(1+\gamma)^{\frac{1}{4}}$ the film totally drys out. Otherwise, the evaporating film only partially dries out and funnels into tapering rivulets in the troughs which steadily thicken. Mass transfer during evaporation is greater for a fluted cylinder than for an unfluted cylinder for relatively short cylinders, but is significantly less for long fluted cylinders due to the dry-out characteristics of the film. Finally, it should be noted that gravity-driven film flows are susceptible to instabilities, even at relatively low flow rates (see, for example, Mei 1966 and Yih 1963), and therefore some care should be taken when applying the results presented here in practical applications.

This work was carried out in the course of research sponsored by the National Science Foundation under grant MSM 85-13795 (R.E.J.) and by support from the Battelle Columbus Labs (A.T.C.) through the Gas Research Institute, Chicago, Illinois.

REFERENCES

GREGORIG, R. 1954 Hautkondensation an Funegewellton Oberflachen bei Berucksichtigung der Oberflachenspannungen. *Z. Angew. Math. Phys.* **5**, 36.

HONDA, H. & FUJII, T. 1984 Semi-empirical equation for condensation heat transfer on vertical fluted tubes. In *Fundamentals of Phase Change: Boiling and Condensation* (ed. C. T. Avedisian & T. M. Rudy), *Winter Annual Meeting of the ASME, New Orleans, LA, 9–14 December 1984.*

JOOS, F. M. 1984 Thin liquid films on arbitrary surfaces with condensation or evaporation. In *Fundamentals of Phase Change: Boiling and Condensation* (ed. C. T. Avedisian & T. M. Rudy), *Winter Annual Meeting of ASME, New Orleans, LA, 9–14 December 1984.*

MEI, C. C. 1966 Nonlinear gravity waves in a thin sheet of viscous fluid. *J. Maths & Phys.* **45**, 266.

MORI, Y., HIJIKATA, K., HUASAWA, S. & NAKAYAMA, W. 1979 Optimized performance of condensors with outside condensing surface. In *Condensation Heat Transfer* (ed. P. J. Marto & P. G. Kroeger), *18th Annual Heat Transfer Conf., San Diego, California, 6–8 August 1979*, p. 55.

NUSSELT, W. 1916 Die Oberflachenkondensation des Wasserdampfes. *Z. Vereines deutscher Ing.* **60**, 569.

OWENS, W. L. 1978 Correlation of thin film evaporation heat transfer coefficients for horizontal tubes. In *Proc. Fifth Ocean Thermal Energy Conversion Conference, Miami, Florida, 20–22 Feb. 1978*, p. VI–71.

PANCHAL, C. B. & BELL, K. J. 1979 Analyses of Nusselt-type condensation on a vertical fluted surface. In *Condensation Heat Transfer* (ed. P. J. Marto & P. G. Kroeger), *18th Annual Heat Transfer Conference, San Diego, California, 6–8 August 1979*, p. 45.

ROTHFUS, R. R. & LAVI, G. H. 1978 Vertical falling film heat transfer: literature summary. In *Proc. Fifth Ocean Thermal Energy Conversion Conference, Miami, Florida, 20–22 Feb. 1978*, p. VI–90.

SIDEMAN, S. & LEVIN, A. 1979 Effect of the configuration on heat transfer to gravity driven films evaporating on grooved surfaces. *Desalination* **31**, 7.

SIDEMAN, S., LEVIN, A. & MOALEM-MARON, D. 1982 Film flow and heat transfer on a vertically grooved surface. In *Proc. Seventh Intl Heat Transfer Conf., Munich* (ed. U. Grigull *et al.*), *V*, 153.

WEBB, R. L. 1979 A generalized procedure for the design and optimization of fluted Gregorig condensing surfaces. *Trans. ASME* C: *J. Heat Transfer* **101**, 335.

WHITHAM, G. B. 1974 *Linear and Nonlinear Waves.* Wiley.

YIH, C. S. 1963 Stability of liquid flow down an inclined plane. *Phys. Fluids* **6**, 321.